Journal of Hydrology: Regional Studies 62 (2025) 102999

Contents lists available at ScienceDirect

Journal of Hydrology: Regional Studies

journal homepage: www.elsevier.com/locate/ejrh

Rethinking water reuse for climate adaptation in Apulia, Italy: From plant-level to system-wide strategies

Matteo Sangiorgio [a,*], Enrico Weber [b], Marco Micotti [b], Andrea Castelletti [a,c]

[a] Department of Electronics, Information and Bioengineering, Politecnico di Milano, Via Ponzio 34/5, Milan, 20133, Italy
[b] SoftWater s.r.l., Via Giuseppe Luosi, 13, Milan, 20131, Italy
[c] RFF-CMCC European Institute on Economics and the Environment, Centro Euro-Mediterraneo sui Cambiamenti Climatici, Via Bergognone, 34, Milan, 20144, Italy

ARTICLE INFO

Keywords:
Water reuse
Circular water economy
Climate change adaptation
Water resources management
Multi-objective analysis

ABSTRACT

Study region: The Apulian Aqueduct (Acquedotto Pugliese) is Italy's largest water distribution system, supplying urban, industrial, and agricultural users across the Apulia region in southern Italy. Apulia is characterized by a predominantly semi-arid Mediterranean climate, where limited local water availability and recurrent droughts exacerbate competition among sectors.

Study focus: This study presents a decision-analytic framework (DAF) for the design of Pareto-efficient, system-wide water portfolios that integrate conventional management and reuse technologies. The DAF jointly evaluates water allocation, reservoir operation, and reuse deployment under historical conditions and four future scenarios combining climate conditions (RCP 4.5 and 8.5) and socio-economic projections.

New hydrological insights for the region: Under future projections, decreasing water availability and growing drinking water demand are expected to intensify conflicts among sectors, challenging the system's capacity to meet supply needs. Historically, irrigation and industrial deficits averaged 56.8 Mm^3/year and drinking water deficits 31.4 Mm^3/year. In the most extreme climate scenario (RCP 8.5, 2090–2099), these increase to 180.4 Mm^3/year (+218%) and 185.9 Mm^3/year (+492%), respectively. Implementing water reuse reduces irrigation and industrial deficits by 29.3 Mm^3/year and drinking deficits by 15.7 Mm^3/year, yet remains far from restoring historical performance. These results demonstrate that while reuse technologies offer meaningful relief, only coordinated, large-scale adaptation strategies can ensure the long-term resilience of Apulia's water system under future climatic stress.

1. Introduction

In recent decades, the Mediterranean region has experienced prolonged warm spells and reduced precipitation, leading to unprecedented droughts (Büntgen et al., 2021; Garrido-Perez et al., 2024). Spain and Italy, the two largest countries in the area, are among the most affected in Europe, with estimated annual economic losses of approximately €1.5 billion and €1.4 billion, respectively—accounting for nearly one-third of total drought losses across the EU and UK, with over 70% impacting agriculture, energy, and domestic water supply sectors (Cammalleri et al., 2020). Climate projections indicate worsening conditions by 2060: projections for the period 2021–2060 show that drought occurrences ranged between 55 and 125 months (i.e., about 12%–25% of

* Corresponding author.
E-mail address: matteo.sangiorgio@polimi.it (M. Sangiorgio).

https://doi.org/10.1016/j.ejrh.2025.102999
Received 7 August 2025; Received in revised form 12 November 2025; Accepted 24 November 2025
Available online 29 November 2025

the 40 years) (Essa et al., 2023); under a +3 °C scenario, damage in the Mediterranean could reach €8 billion/year, effectively doubling current losses (Cammalleri et al., 2020). In this context, water reuse is, and will be in the future, essential to mitigate the impacts of droughts and alleviate water scarcity (Hristov et al., 2021; Kahn et al., 2025). Yet, this practice is still far below its potential in many Mediterranean countries. For instance, in Italy , only 4% of treated wastewater, around 200 Mm^3/year, is reused, far below the estimated 23% potential (ARERA, 2020). Barriers include high capital costs, fragmented regulatory frameworks, and low public acceptance (Neri et al., 2024). Effective water reuse requires integrated planning. Reuse strategies need to be coordinated with existing infrastructure (e.g., irrigation networks, aquifers), employ modular treatment technologies suited to target users, and be supported by adaptive policies and stakeholder engagement (EU Water Directors, 2016; Zaniolo et al., 2023). Yet, reuse initiatives are often designed in isolation, focusing on individual plant performance rather than system-wide synergies (Rizzo et al., 2020; Ahmed et al., 2022; Penserini et al., 2024).

In this paper, we introduce a Decision Analytic Framework (DAF) for designing efficient water portfolios that integrate water reuse with the operation of other infrastructures in urban and peri-urban water systems. The framework identifies Pareto-efficient portfolios and assesses their robustness under varying climatic and socio-economic futures.

Several studies have adopted DAFs based on multi-objective optimization to design efficient water portfolios by integrating planning and management strategies. Applications include dam siting and sizing (Bertoni et al., 2020; Hatchard et al., 2023), financial risk management (Hamilton et al., 2022), joint design of hydraulic infrastructure and irrigation districts (Giuliani et al., 2022), inter-basin water transfer policy design (Valerio et al., 2023), and operational space definition (Huang et al., 2025). However, to the best of our knowledge, no study has yet extended this approach to the integrated planning of water reuse infrastructure.

We apply the DAF to a case study in the Apulia region of southern Italy. Apulia is characterized by a water-scarce hydrological regime, a vast and highly interconnected distribution network (the Apulian aqueduct), and diverse, often competing, demands from agricultural, industrial, and domestic users. These factors make the management of its regional water system particularly complex and challenging (Lopez and Vurro, 2008; De Girolamo et al., 2022; Sangiorgio et al., 2022; Corbari et al., 2024). The current system relies on conventional water sources, including five artificial reservoirs, two major natural springs, and several well fields. To enhance resilience under increasing drought pressure, regional authorities are considering two complementary reuse strategies: (i) upgrading existing wastewater treatment plants with advanced treatment lines to recover wastewater for agricultural irrigation, and (ii) reactivating decommissioned wells by improving water quality through modular treatment technologies. In this study, we assess the potential benefits of these reuse measures by integrating them into the existing water system and quantifying their impacts across key sectors—irrigation, industrial use, and drinking water supply. The analysis spans both a historical baseline decade and multiple future scenarios that combine varying patterns of water availability and demand.

2. Materials and methods

2.1. The Apulian water system

The Apulia region, located in southern Italy, spans an area of approximately 19,500 km^2 and exhibits a predominantly semi-arid climate, characterized by hot, dry summers and mild winters (Polemio and Lonigro, 2015). Annual precipitation ranges from 400–600 mm in most areas, occasionally reaching 1000 mm in the northern subregion (Todorovic, 2007). Hydrological patterns are highly irregular, with elevated flows in winter and negligible runoff during summer months. The region's only significant rivers, Fortore and Ofanto, are confined to its northern portion.

The scarcity of surface water across much of Apulia led to the construction of the Apulian aqueduct (1906–1939), Italy's largest water distribution system (WDS), which supplies the region from water-rich basins in neighboring areas (Fig. 1). The primary sources, located outside or near Apulia's borders, include natural springs (about 29% of supply, mainly Sele and Calore in Campania) and dammed hydrological basins (over 50%). Major reservoirs include Occhito (Fortore River), Conza (Ofanto River), Locone, Pertusillo (Agri River), and Monte Cotugno (Sinni River). In addition, over 200 wells supplement surface water, particularly during drought periods. Managed by the Apulian Aqueduct Company (AQP), the system comprises more than 20,000 km of interconnected networks with a transport capacity exceeding 790 Mm^3/year.

AQP operates all water adduction, storage, purification, and distribution services for domestic, agricultural, and industrial sectors. Drinking water is supplied to over 4.5 million residents (including several municipalities in neighboring regions). Irrigation water is distributed across six large districts (Gardano, Capitanata, Terre d'Apulia, Stornara e Tara, Arneo, and Ugento Li Foggi), while the Monte Cotugno reservoir also supplies the Taranto industrial area, home to one of Europe's largest steel manufacturing facilities.

2.2. Decision analytic framework

The Decision Analytic Framework (DAF), illustrated in Fig. 2, integrates reuse technologies within water system operations to derive efficient and robust water portfolios. It couples a strategic simulation model with an optimization engine to compute Pareto-efficient portfolios under varying climatic and socio-economic scenarios. The framework evaluates three key performance indicators (irrigation and industrial deficit, drinking supply, and cost associated to drinking water distribution) across multiple (historical and future) scenarios.

We adopt the Evolutionary Multi-Objective Direct Policy Search (EMODPS) approach, a simulation-based optimization method that couples direct policy search with multi-objective evolutionary algorithms (Giuliani et al., 2017; Quinn et al., 2019; Giuliani et al., 2021). Rather than optimizing a sequence of system decisions, EMODPS searches the parameters of operating policies that

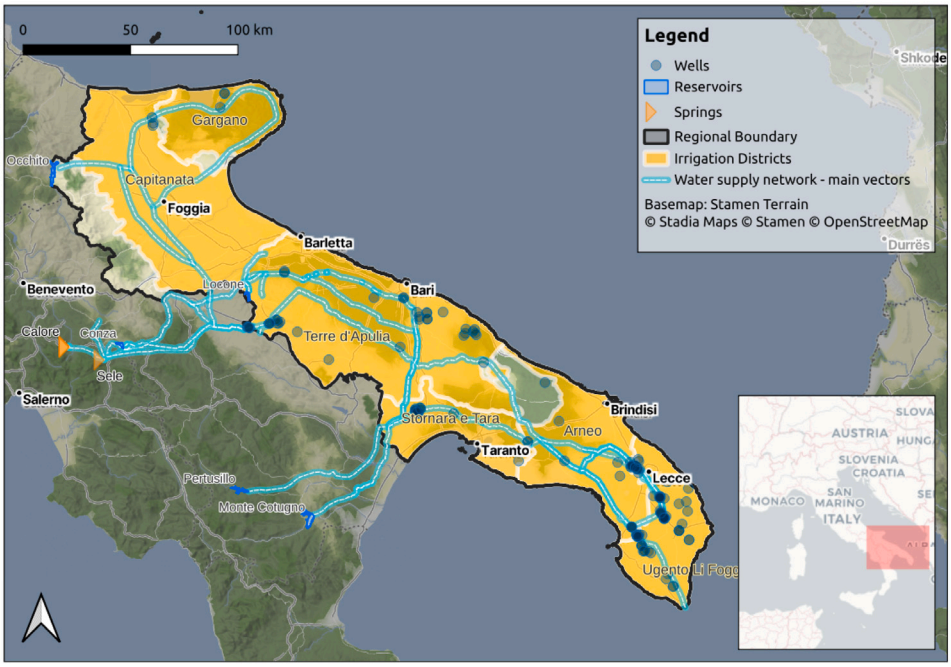

Fig. 1. Map of the Apulia water system.

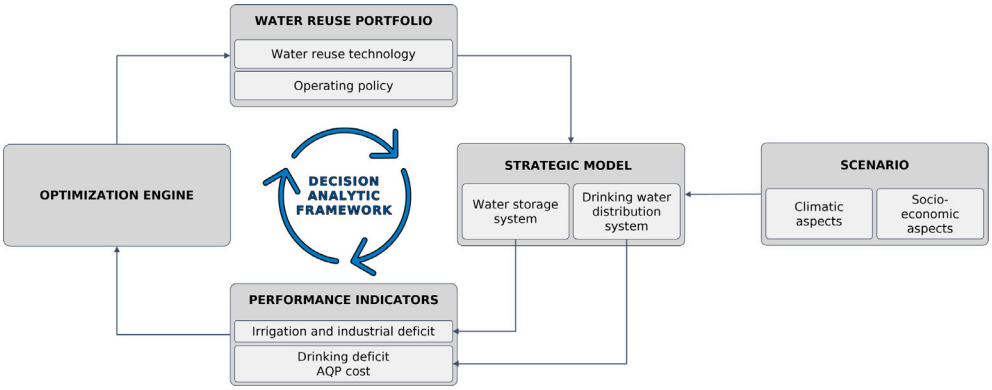

Fig. 2. Workflow of the Decision Analytic Framework (DAF) for identifying efficient water reuse portfolios.

map system states (e.g., reservoir storage, time of year) to control actions (e.g., reservoir releases, extractions from wells). This formulation allows the identification of adaptive strategies that can respond dynamically to changing conditions. This approach provides a coherent framework for integrating planning decisions, such as water reuse adoption, with operational control of the water system.

2.2.1. Strategic water system model

The simulation model represents two main components: the water storage system and the distribution network (Fig. 3, left panel). Five reservoirs (Occhito, Conza, Locone, Pertusillo, and Monte Cotugno) supply irrigation districts and, in the case of Monte Cotugno, also the Taranto industrial area. Drinking water is sourced from two natural springs (Sele and Calore) and several well fields. The distribution network connects over 250 nodes, including hydroelectric plants, pumping stations, and purification facilities.

The daily dynamics of each reservoir (Fig. 3, right panel) is modeled using mass balance equations:

$$s_{t+1} = s_t + q_{t+1} - r_{t+1},$$

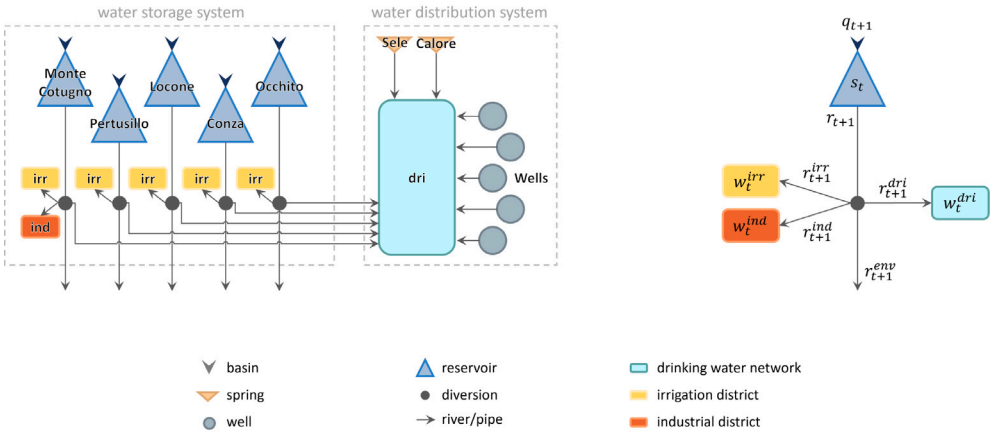

Fig. 3. Topological scheme of the Apulian water system (left) and a single-reservoir sub-model (right). A detailed mathematical formulation is provided in Appendix B.

Table 1
Annual volumes of reclaimed wastewater for each irrigation and industrial district.

Use	Reservoir	Volume [Mm^3/year]
Irrigation	Occhito	31.54
Irrigation	Locone	3.94
Irrigation	Conza	1.26
Irrigation	Pertusillo	5.68
Irrigation	Monte Cotugno	6.94
Industrial	Monte Cotugno	12.61

where s_t is storage, q_{t+1} is net inflow, and r_{t+1} is release. The water released is allocated among (irrigation, industrial, and drinking) sectors via a regulated diversion mechanism (Celeste and Billib, 2009). Each diversion is defined by a couple of parameters: α and β (the parameter vectors $\boldsymbol{\alpha}$ and $\boldsymbol{\beta}$ contain the respective parameters for all the diversions).

The decisions on the reservoirs releases ($\mathbf{u}_t$) and the total amount of water drawn from the well fields (u_t^w) are computed by system's operating policy, $\mathbf{p}(\cdot)$, that is parametrized using radial basis functions (RBFs) as in previous applications in reservoir management (Giuliani et al., 2014; Salazar et al., 2024). $\mathbf{p}(\cdot)$ depends on a set of parameters (θ), and takes in input information on the current state of the water system (i.e., day of the year and reservoir storage).

The WDS (light blue block in Fig. 3, left panel) is simulated using Aquator, a proprietary software developed by Water Resource Associates and Oxford Scientific Software Ltd used by AQP for the daily WDS operation. Aquator represents around 500 physical arcs (i.e., pipes and channels), each characterized by a certain flow, and around 250 nodes, in which the water balance is computed. Even if Aquator can compute the drinking water deficits and the distribution cost relative to the drinking sector, because of its real-time to run-time ratio (a simulation on a one-year horizon requires a computing time of approximately one hour), it cannot be used in simulation-based optimizations involving millions of runs such as EMODPS. To overcome this limitation, we replaced Aquator with a high-fidelity surrogate model identified to reproduce its behavior. The surrogate consists of a feed-forward artificial neural network with nine inputs (five reservoir releases, two spring inflows, one aggregated well input, and total drinking demand) and two outputs (drinking deficit and distribution cost). The training dataset, comprising over 150,000 Aquator simulations, was designed to cover a wide range of operating conditions of the water distribution system. The final network architecture includes a single hidden layer with eight neurons and achieved $R^2 > 0.98$ across training, validation, and test sets, ensuring negligible loss of accuracy and enabling its safe integration into the optimization framework (details in Appendix A).

2.2.2. Water reuse portfolios

Beyond decisions on daily water volumes released from each reservoir, extracted from wells, and allocated to the various water users (as introduced in the previous section and detailed in Appendix B), a defining feature of a water portfolio lies in the strategic choice regarding the adoption of innovative water reuse technologies.

We consider two possible alternatives: (i) the current situation, where no advanced water reuse technologies are implemented, and (ii) a scenario where multiple reuse actions are adopted. Specifically, two wastewater reclamation plants are considered, capable of recycling a total annual volume of 61.97 Mm^3/year—of which 49.36 Mm^3/year is allocated for agricultural use and 12.61 Mm^3/year for industrial use (Table 1).

In addition, up to 9.45 Mm^3/year can be extracted from seven well fields that were previously decommissioned due to groundwater quality degradation (Table 2).

Table 2
Annual water volumes available from the reactivation of decommissioned wells.

Location	Volume [Mm^3/year]
Cerignola	0.63
Andria	0.63
Bari	0.63
Lecce	0.63
Taranto	0.63
Parco del Marchese	3.15
Opera 3	3.15

It is important to emphasize that, although the design of reservoir operation strategies and the planning of water reuse technologies have traditionally been addressed as separate problems, they are inherently interconnected. To maximize the benefits of water reuse adoption, a tailored management of the entire water system is required, ensuring coordination with all other components (e.g., reservoirs, wells, diversions, etc.).

2.2.3. Climatic and socio-economic scenarios

Simulating the system requires defining scenarios that quantify input variables affecting system dynamics:

- Reservoir inflows and natural spring streamflows;
- Irrigation, industrial, and drinking water demands;
- Supply, treatment, and distribution costs per unit flow.

Historical data (2010–2019) are used to define the baseline scenario, while robust identification of water portfolios requires generating plausible future projections.

Hydro-meteorological aspects. Climate variability, which defines future hydro-meteorological regimes, is modeled using the projections from the IPCC Fifth Assessment Report. We consider two Representative Concentration Pathways (RCPs): RCP 4.5, a moderate scenario, and RCP 8.5, an extreme scenario for worst-case analyses, evaluating mid-century (2050–2059) and end-of-century (2090–2099) conditions. An in-depth description of future hydrometeorological scenarios is provided in Appendix C.

Socio-economic aspects. Future socio-economic developments will influence drinking water demand patterns. The Apulian Water Authority forecasts significant increases in water demand along the coastline, particularly during summer, due to tourism growth, while some rural areas are expected to experience declining demands. The projected annual increase is 80.9 Mm^3, approximately 17% of the region's current drinking water demand.

We therefore define four future scenarios combining two RCPs (4.5 and 8.5) and two future periods (2050s and 2090s), all of them assuming the projected drinking demand.

2.2.4. Performance indicators

Stakeholder interests are captured by a three-dimensional vector **J** of performance indicators to be minimized:

- **Irrigation and industrial deficit**: squared positive deviations between water demand and supply in agricultural districts and the industrial district served by the dams in the system. A quadratic formulation is adopted to penalize concentrated, intense shortages more severely than small, distributed ones for the same deficit volume, reflecting the greater tolerance of these sectors to moderate water stress over time and their higher vulnerability to acute supply disruptions;
- **Drinking water deficit**: positive deviations between water demand and supply across all drinking water consumption centers. Since drinking water provision must satisfy demand almost entirely at all times (shortages being acceptable only under exceptionally severe dry spells) deficits are treated linearly. Any unmet demand must be compensated through alternative sources (e.g., emergency tank-truck supply), making even small deficits operationally significant;
- **Cost**: associated with the supply, treatment, and distribution of drinking water. Only these costs are considered, as reliable estimates for irrigation and industrial supplies are not available; these sectors largely rely on low-energy, gravity-fed conveyance systems with negligible treatment requirements and are therefore assumed to be cost-neutral within this analysis.

Each indicator aggregates performance over a 10-year horizon. As previously discussed, due to the high computational demands of Aquator, the two drinking water sector indicators are computed using a high-fidelity surrogate model.

2.2.5. Optimization engine

The optimal operation of this complex water system involves deciding, at each time step, the volumes to release from reservoirs and extract from aquifers, and their allocation across sectors. The decision variables include parameters governing diversion mechanisms (see Eq. (B.2)) and the operating policies of reservoirs and wells.

The combined parameter set, $\Theta = [\theta, \boldsymbol{\alpha}, \boldsymbol{\beta}]$, defines the optimization problem:

$$\Theta^* = \arg\min_{\Theta} \mathbf{J}_{\Theta}, \tag{1}$$

subject to strategic model constraints.

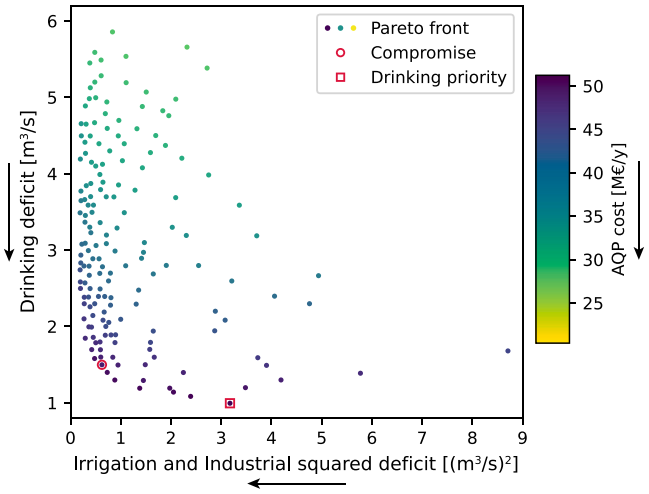

Fig. 4. Pareto-optimal water portfolio performance under the baseline scenario (2010–2019): irrigation and industrial squared deficit (horizontal axis), drinking deficit (vertical axis), and AQP cost (color scale). All indicators must be minimized. The compromise solution is highlighted with a red circle, and the one prioritizing the drinking sector with a red square. Arrows indicate the preferred direction (all performance indicators are costs or deficits to be minimized).

This optimization problem, formulated within the EMODPS framework, is addressed by Multi-objective evolutionary algorithms (MOEAs), which have proven particularly effective for complex water reservoir management problems involving multiple objectives, stochasticity, and non-derivable relationships. These algorithms are iterative procedures that optimize a population of candidate solutions through evolutionary operators: selection, crossover, mutation, and elitism (Guariso and Sangiorgio, 2020; Alhijawi and Awajan, 2024). Starting from an initial population, individuals (i.e., parameterizations Θ) are refined based on a fitness function defined by the performance indicators ($\mathbf{J}_\Theta$). Here, we employ the self-adaptive Borg MOEA (Hadka and Reed, 2013), which has demonstrated high robustness in similar contexts (Salazar et al., 2016).

3. Results

We applied the DAF using a historical baseline scenario and four future scenarios that combine two RCPs (4.5 and 8.5) with two future periods (the 2050s and 2090s), incorporating the projected 17% increase in drinking demand. Each future scenario was evaluated both with and without the implementation of water reuse technologies.

3.1. Historical baseline

Fig. 4 reports the performance indicators obtained with the Pareto-optimal water portfolios for the historical baseline. Portfolios that belong to the Pareto front are characterized by the fact that no other configuration can improve one indicator without worsening at least one of the others. The collection thus represents the most efficient trade-offs achievable given system constraints. Points in the upper left corner with a light color represent portfolios that minimize irrigation and industrial deficits as well as AQP costs, while accepting relatively high drinking deficits. Conversely, points in the lower right corner with a darker color correspond to portfolios achieving very low drinking deficits, but at the expense of substantially higher irrigation and industrial deficits and higher AQP costs. These two extremes illustrate the opposite ends of the trade-off space, while the shape of the Pareto front between them reflects the strength of the conflict among objectives. If the two extremes were connected by a straight front, it would indicate a constant trade-off, where an improvement in one objective is offset by a proportional deterioration in another. In contrast, the convex shape observed here reveals a much sharper trade-off: small improvements in one indicator require large sacrifices in another. This pattern indicates that, under the historical conditions, strong conflicts exist among water sectors because the drought-prone hydro-meteorological regime of the region does not provide sufficient water volumes to satisfy all demands simultaneously, thereby triggering competitive use of water resources. The drinking water sector experiences limited deficits only at the cost of considerable expenses for water distribution, pumping, and treatment. Conversely, high deficits correlate with lower economic costs, as less water is circulated through the system. This trade-off arises because the substantial flow of water into the distribution network drives purification and pumping expenses. Revenue from the four small hydropower plants offers only limited mitigation of these costs.

Among the Pareto-efficient portfolios, we selected the one most aligned with current water management practices. Discussions with decision-makers revealed that the existing strategy prioritizes addressing the drinking water deficit (red square in Fig. 4) over irrigation-industrial deficits (Formally, we selected the solutions whose drinking water deficit was within 1% of the best-performing solution, and within this subset, we chose the one achieving the best performance for irrigation and industrial deficits). This practice

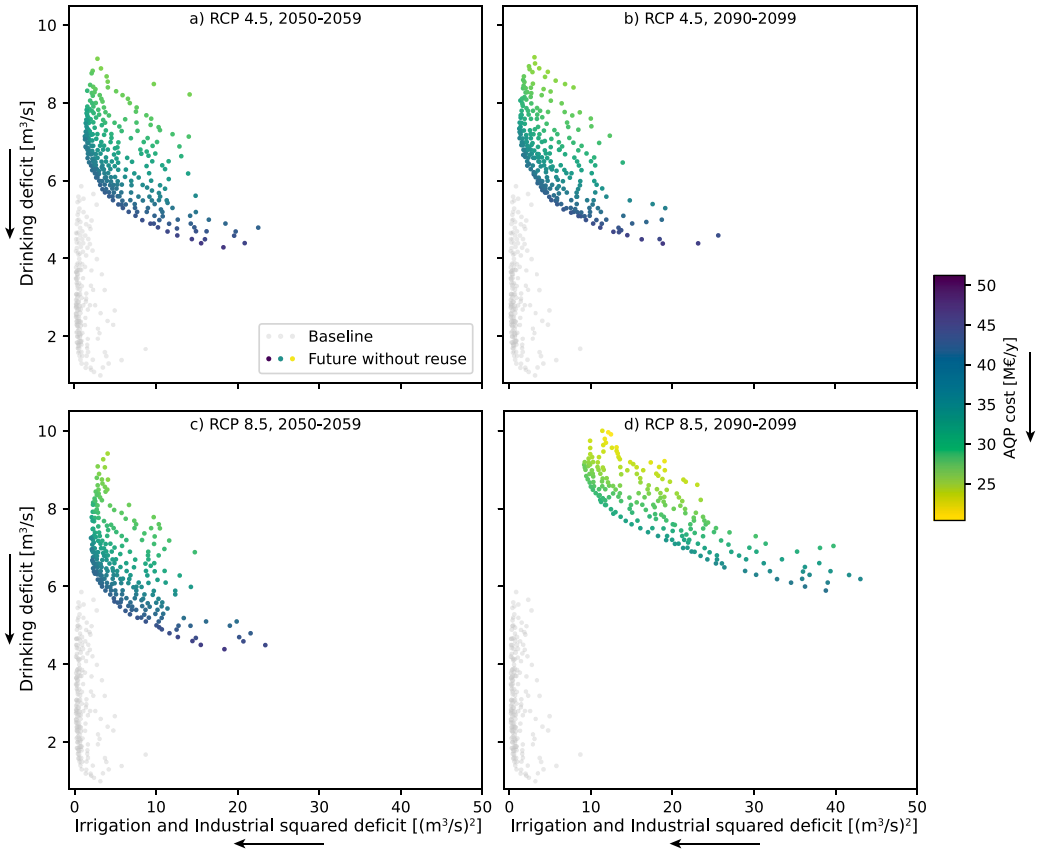

Fig. 5. Pareto-optimal water portfolio performance under future scenarios without water reuse: (a) RCP 4.5 for 2050–2059, (b) RCP 4.5 for 2090–2099, (c) RCP 8.5 for 2050–2059, and (d) RCP 8.5 for 2090–2099. The Pareto front of the baseline scenario is shown in gray for comparison. Arrows indicate the preferred direction (all performance indicators are costs or deficits to be minimized).

is common in regions affected by water scarcity, as interruptions in civil water supply are considered unacceptable and often mitigated by costly measures, such as bottled water distribution or tank deliveries to urban centers. In contrast, the costs borne by AQP are treated as secondary indicators in the decision-making process because they are ultimately passed on to end-users via utility bills. Nevertheless, including these costs in the optimization is critical to ensure the algorithm seeks the least expensive allocation strategy for given deficit levels. Although we did not account for the capital and operational costs of implementing innovative reuse technologies, such estimates are highly contingent on future legislative and technological developments, which cannot be reliably anticipated at this stage. For comparison, we also present a potential compromise portfolio (red circle in Fig. 4) that balances deficits across sectors. Formally, we selected the solutions whose drinking water deficit was within 10% of the best-performing solution, and within this subset, we chose the one achieving the best performance for irrigation and industrial deficits. This results in a solution closer to the point of maximum curvature of the baseline Pareto front. However, it is worth stressing that this solution does not fully align with current operational priorities.

A key feature of the proposed framework is its centralized approach to identifying Pareto-efficient portfolios, which assumes that a single water authority can oversee reservoir releases, allocate resources among users, and manage system operations to comprehensively explore trade-offs between competing sectoral demands and identify suitable compromises, typically favoring the drinking water sector. The assumption of centralized management offers a plausible representation of current practices: at the beginning of each irrigation season, negotiations between stakeholders and water authorities are held to coordinate resource allocation and establish acceptable compromises. Obviously, the use of water resources in a context of scarcity is by definition competitive, but the actors involved agree on an allocation strategy to avoid individual behaviors that could be harmful to the community (and ultimately to the individuals themselves, as illustrated by the tragedy of the commons). Within this context, the framework can serve as a valuable analytical tool to support such negotiations by providing quantitative insights into alternative management strategies and enabling informed, data-driven decisions. In particular, while current negotiations are typically based on the definition of total seasonal water volumes assigned to each sector, the proposed framework allows for a more advanced and quantitative approach. By relying on the Pareto frontiers generated through the simulation, decision-makers could identify an efficient daily allocation corresponding to the selected trade-off between competing objectives. This would make it possible to move from a single, season-wide allocation decision toward a dynamic strategy that efficiently distributes water on a day-to-day

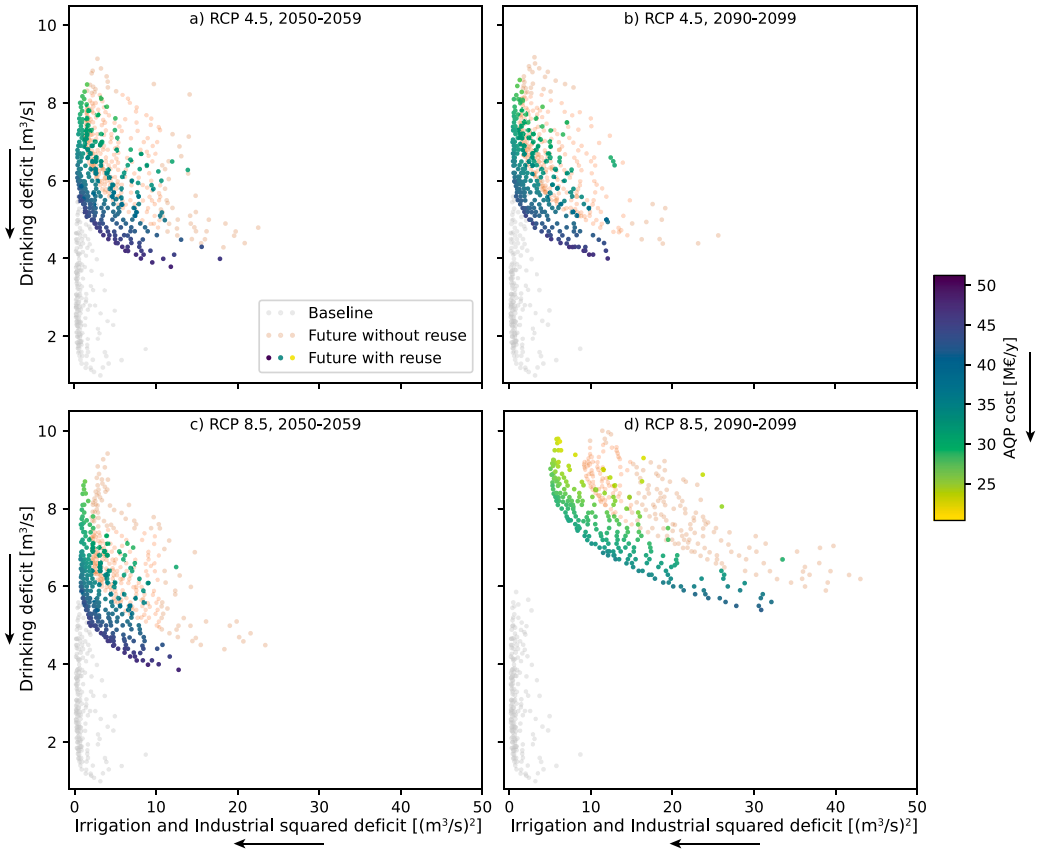

Fig. 6. Pareto-optimal water portfolio performance under future scenarios with water reuse: (a) RCP 4.5 for 2050–2059, (b) RCP 4.5 for 2090–2099, (c) RCP 8.5 for 2050–2059, and (d) RCP 8.5 for 2090–2099. The Pareto front of the baseline scenario is shown in gray, and those of future scenarios without reuse are shown in orange. Arrows indicate the preferred direction (all performance indicators are costs or deficits to be minimized).

basis. In addition, the framework enables the execution of what-if analyses on relevant aspects — such as future climatic and socio-economic scenarios or the adoption of water reuse technologies and other infrastructural measures — while still ensuring that the daily allocations remain efficient. In this way, the tool not only supports the coordination among stakeholders but also provides a robust analytical basis for planning and managing water resources under changing conditions.

3.2. Future scenarios

Under future hydro-meteorological conditions without water reuse, reduced water availability combined with increased demand will considerably strain the Apulian water system (Fig. 5). System performance is expected to deteriorate significantly (all Pareto fronts shift upward and rightward), with future portfolios entirely dominated by their baseline counterparts (gray points). Two distinct clusters emerge: one representing moderate climate change (RCP 4.5 and RCP 8.5 for 2050–2059, and RCP 4.5 for 2090–2099; panels a–c), and another reflecting extreme climate change (RCP 8.5 for 2090–2099; panel d). This pattern is consistent with the projected radiative forcing trajectories: RCP 4.5 stabilizes around 4.5 W/m^2 by mid-century, whereas RCP 8.5 increases from 5 W/m^2 (2050–59) to 8.5 W/m^2 by 2100 in the absence of mitigation efforts. All scenarios impose unsustainable pressures on freshwater resources, exacerbating conflicts between sectors (future Pareto fronts are more stretched than the baseline, especially along the irrigation-industrial deficit axis).

Reuse technologies have a positive effect: all Pareto-efficient portfolios shift toward the lower-left corner compared to their future counterparts without reuse (orange points in Fig. 6). However, they still fall short of bridging the gap to the baseline (gray points). In moderate climate change scenarios, water reuse allows irrigation deficits comparable to the baseline and, if prioritized, their near-complete elimination. Drinking water deficits, however, remain considerably higher than historical values. Under extreme climate change, deficits increase substantially across all sectors, even with reuse measures.

Focusing on policies that prioritize the drinking sector, irrigation and industrial deficits (Fig. 7, top) increase from 56.8 Mm^3/year to 112.2–118.3 Mm^3/year (+97%–108%) in moderate scenarios, and to 180.4 Mm^3/year (+218%) in the extreme scenario. Water reuse reduces these deficits by 32.3–36.6 Mm^3/year (−29%) in moderate cases and by 29.3 Mm^3/year (−16%) under extreme

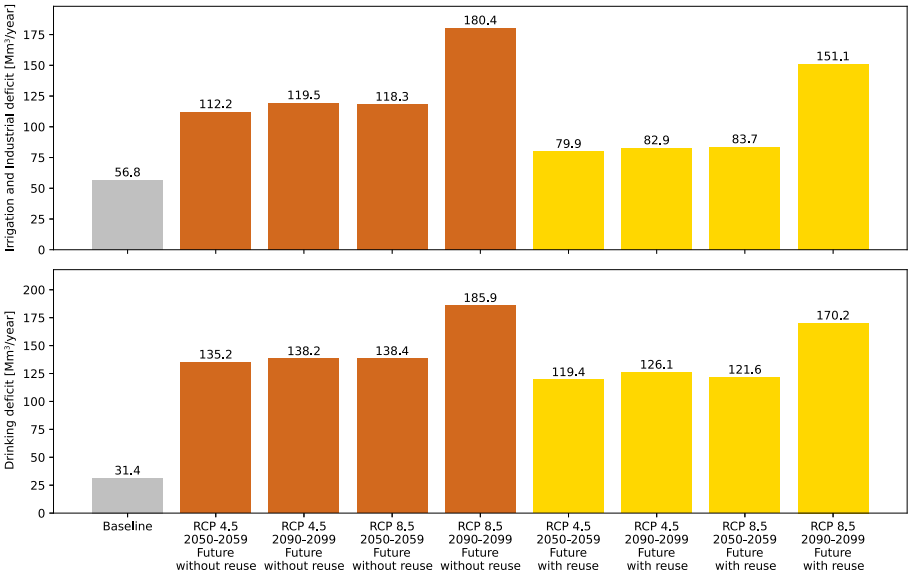

Fig. 7. Annual water deficits (irrigation and industrial on top; drinking water on bottom) for baseline (gray) and future scenarios without (orange) and with (yellow) water reuse, based on policies prioritizing the drinking sector.

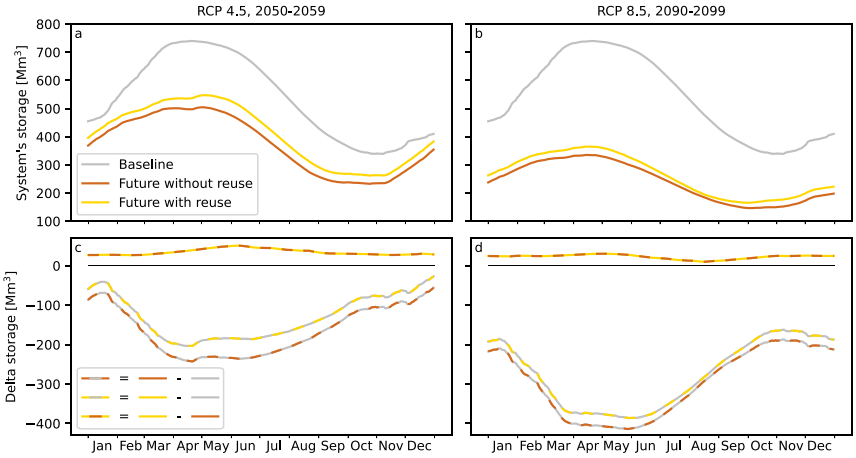

Fig. 8. Average water storage in Apulian reservoirs (aggregate across five reservoirs) for RCP 4.5 (2050–2059; a) and RCP 8.5 (2090–2099; b). The historical baseline (gray) is compared with future trajectories without (orange) and with (yellow) water reuse. Panels (c) and (d) show the differences between trajectories in panels (a) and (b).

conditions. The drinking sector, despite being prioritized, faces even larger challenges (Fig. 7, bottom). In moderate scenarios, potable water deficits quadruple from 31.4 Mm^3/year to 135.2–138.4 Mm^3/year (+330%–341%), and rise nearly sixfold to 185.9 Mm^3/year (+492%) under extreme climate change. Water reuse offers only partial mitigation (15 Mm^3/year), significant in absolute terms but limited relative to the scale of future challenges.

The framework also allows in-depth analysis of system variables. Fig. 8 presents the mean cyclostationary trend of total water storage across all reservoirs, serving as a proxy for resource availability and system stress. In the baseline, average storage is 538.5 Mm^3, with a pronounced seasonal pattern peaking in late spring at 740.2 Mm^3 (preparation for irrigation season) and dipping to 339.2 Mm^3 at the end of summer. In moderate future scenarios (RCP 4.5 for 2050–2059), average storage declines to 374.1 Mm^3 (−30.5%), partially mitigated by reuse strategies to 408.9 Mm^3 (+34.8 Mm^3 relative to no-reuse cases). Under extreme scenarios (RCP 8.5 for 2090–2099), storage drops to 240.1 Mm^3 (−55.4%), with reuse raising it to 262.6 Mm^3.

4. Conclusion

This study presents a novel decision-analytic framework to evaluate the role of innovative water reuse technologies as climate change adaptation measures within complex regional water systems. Unlike traditional approaches that assess reuse plants in

isolation, our framework integrates their operation with existing hydraulic infrastructure — including reservoirs, wells, and extensive distribution networks — allowing for system-level quantification of their impact on user satisfaction and resource resilience. This paradigm shift provides critical insights for policymakers and practitioners seeking to move beyond plant-centric designs toward coordinated, adaptive water management strategies.

Applying the framework to the Apulian water system — a representative case of drought-prone Mediterranean regions with intricate infrastructure and competing sectoral demands — highlights the profound challenges posed by climate and socio-economic change. Future hydro-meteorological scenarios project a substantial reduction in freshwater availability, exacerbated by rising drinking water demand driven by coastal urbanization and tourism. While advanced reuse interventions, such as wastewater reclamation and reactivation of decommissioned wells, significantly alleviate system stress, they remain insufficient to fully restore historical performance levels. This underscores the urgency of pursuing additional adaptation strategies, including large-scale infrastructural investments such as seawater desalination and transboundary water transfers, to secure the region's long-term water security.

Importantly, the proposed framework extends beyond technical analysis. By enabling the systematic identification of Pareto-efficient water portfolios, it provides a robust decision-support tool for navigating trade-offs between competing uses. This capability is particularly relevant in contexts where water allocation decisions require negotiation among diverse stakeholders. Through quantitative representations of alternative management pathways, the framework fosters informed, transparent, and data-driven decision-making processes. These findings resonate with emerging European policies advocating for the integration of circular water economy principles into regional planning (see, for instance, the European Water Resilience Strategy from the Directorate-General for Environment, 2025, and the opinion factsheet from the Commission for the Environment, Climate change and Energy, 2025). The approach offers a scalable and adaptable template for other regions worldwide facing similar vulnerabilities, contributing to the global agenda of sustainable and climate-resilient water management.

CRediT authorship contribution statement

Matteo Sangiorgio: Writing – review & editing, Writing – original draft, Software, Formal analysis, Data curation. **Enrico Weber:** Writing – review & editing, Software, Formal analysis, Data curation, Conceptualization. **Marco Micotti:** Writing – review & editing, Software, Formal analysis, Data curation, Conceptualization. **Andrea Castelletti:** Writing – review & editing, Supervision, Project administration, Funding acquisition, Conceptualization.

Funding information

The work has been partially funded by the European Commission under the Project Ô project belonging to the Horizon 2020 research and innovation program (grant no. 776816).

Declaration of competing interest

The authors declare the following financial interests/personal relationships which may be considered as potential competing interests: Matteo Sangiorgio reports financial support was provided by Horizon Europe. If there are other authors, they declare that they have no known competing financial interests or personal relationships that could have appeared to influence the work reported in this paper.

Acknowledgment

The authors would like to thank Luciano Venditti, who is responsible for the large distribution networks and reservoirs (Grandi Vettori e Serbatoi) area of AQP.

Appendix A. Surrogate model identification

The drinking water distribution network managed by AQP is currently modeled through the Aquator toolbox, developed by Water Resource Associates and Oxford Scientific Software Ltd. Aquator could be nested into the strategic model to derive the drinking sector indicator, i.e., drinking water deficit and associated distribution cost. Yet, this approach would incur impractical computational expenses, taking over 4000 days for a 10-year horizon in our optimization setting.

A common workaround is the use of a surrogate modeling technique (Castelletti et al., 2011; Razavi et al., 2012; Guariso and Sangiorgio, 2019; Han et al., 2023; Sun et al., 2023). A surrogate model, sometimes named response surface, emulator, or reduced model, is a lower-order, computationally faster replica of the original high-fidelity model. The surrogate model directly focuses on the relationship between some input variables and a set of variables of interest (the outputs), rather than providing a detailed description of the physical processes. In the case at hand, the water released into the aqueduct and the drinking water demand represent the surrogate inputs, while the corresponding drinking water deficit and distribution costs are its output (Sangiorgio et al., 2022). The approach requires generating a dataset of input–output samples that are then used to identify the surrogate.

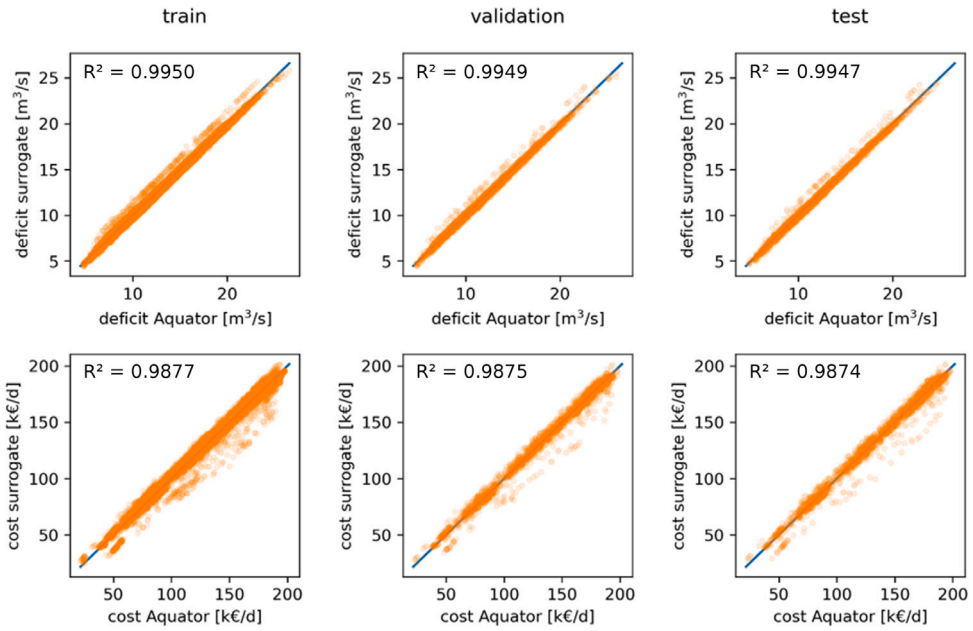

Fig. A.9. Comparison between Aquator simulation and corresponding approximation (i.e., computed with the same inputs) by the surrogate model. The drinking water deficit is on top, and the distribution cost is at the bottom. The dataset is split into training (left), validation (center), and test (right) subsets. Perfect estimations lie on the diagonal (blue line), that is, the set of all points for which the Aquator output is equal to the surrogate estimation.

Dataset generation

The input–output dataset is generated via the design of experiments (appropriate sampling of the input space) and simulation of the original high-fidelity model. To exhaustively sample the multidimensional input space, we consider two sets:

- a regular grid formed by all the combinations of 4 values for each input variable (minimum and maximum as extreme values, plus two intermediate values representative of the variability of the historical probability density function);
- an irregular set of points corresponding to the centroids obtained by clustering the historical data through the mean-shift algorithm.

The regular grid covers the whole input hyperspace, ensuring that the surrogate model does not have to work outside the calibration range (extrapolation). Conversely, the irregular set forces the surrogate model to improve its accuracy in the most significant input space areas (events frequently occurring in the past are more likely to occur in the future as well). Feeding the input dataset defined so far, we run multiple parallel simulations of Aquator (resulting in 158,151 points corresponding to the input defined in the regular grid and the irregular set) to compute the target output to be used for the surrogate identification.

Training, validation, and test

Once the dataset of input–output pairs is available, we have to select a suitable architecture for the surrogate. Machine learning models, such as Artificial Neural Networks (ANNs), are usually used for their flexibility and high performance in terms of accuracy and computing time. Here, we adopt a feed-forward structure with 9 inputs (5 water flows from the reservoirs, 2 from the natural springs, and 1 from all the wells, plus 1 representing the aggregated drinking water demand) and 2 outputs (drinking water deficit and distribution cost for the whole system). The neural network is first implemented in Python (using Keras, a high-level open-source library by Chollet et al. (2015) that provides built-in functions for building neural architectures and auto-differentiation algorithms for their training) and then redefined in native C++ consistently with the main routine for simulation and optimization to avoid the use of a wrapper which would unavoidably slow down the execution.

We split the dataset into training (70%, 110,705 samples), validation (15%, 23,723 samples), and test sets (15%, 23,723 samples). The training set is used to compute the gradients of the model's parameters (weights and biases) during the optimization. The validation set is used to monitor the risk of overfitting and select the hyperparameters (training algorithm, non-linear activation function, batch size, learning rate, number of hidden layers, and number of neurons in the hidden layers), adopting an exhaustive grid search. The test is used to assess the model's accuracy and to check the absence of overfitting on the training or validation data.

The selected neural net has a single hidden layer of 8 neurons with rectified linear units as an activation function. The model was trained for 2000 epochs using Adam optimizer as a training algorithm (Kingma and Ba, 2014), a learning rate equal to 0.001, and

batches of 512 samples. This simple architecture is computationally very efficient and also guarantees high accuracy as demonstrated by the nearly perfect alignment on the diagonal in all the scatter plots of Fig. A.9 and the R^2 values close to 1. In addition, the performance obtained on training, validation, and test sets is constant, proving that the neural network has a high generalization capability (absence of overfitting).

Overall, the results show that the considered neural model is a highly reliable surrogate of the original aqueduct simulation model. We can thus safely replace the original implementation with its surrogate in the strategic modeling framework to ensure the feasibility of the optimization task. Naturally, with the surrogate model, internal compensations are allowed between deficits at different points of the network. Furthermore, it is not possible to carry out detailed analyses at the level of the internal components, as well as of the individual demand centers.

Appendix B. Water system model

The dynamics of each reservoir (Fig. 3, right) is described through the daily balance equation of its storage:

$$s_{t+1} = s_t + q_{t+1} - r_{t+1}, \tag{B.1}$$

where s_t is the storage at time t, q_{t+1} is the net water inflow (i.e., inflow minus evaporation and other minor losses such as infiltration) in the interval $[t; t+1)$, and r_{t+1} the water released over the same interval.

The release is defined by a non-linear, stochastic relation between the release decision (u_t) and the actual release, $r_{t+1} = f(s_t, u_t, q_{t+1})$ (Soncini-Sessa et al., 2007). u_t is determined by an operating policy based on the current state of the system (i.e., day of the year and reservoir storage). The actual release is generally equal to the release decision unless the prescribed release lies outside the minimum and maximum allowable releases (if there is insufficient water to meet the prescribed release or if the prescribed release would result in spillage).

The water released is distributed to the different users through a regulated diversion mechanism (Celeste and Billib, 2009). The volume of water diverted to agricultural districts, industries, and the aqueduct are r^{irr}_{t+1}, r^{ind}_{t+1}, and r^{dri}_{t+1} and should ideally meet the corresponding water demands. For example, the water diverted to the irrigation district is calculated as follows:

$$r^{irr}_{t+1} = \begin{cases} \min\left(w^{irr}_t \cdot \left(\frac{r_{t+1}}{\alpha}\right)^{\beta},\ r_{t+1}\right) & \text{if } r_{t+1} \le \alpha \\ \min\left(w^{irr}_t,\ r_{t+1}\right) & \text{otherwise,} \end{cases} \tag{B.2}$$

where α and β are the parameters of the diversion mechanism. The same approach is used to divide the remaining water flow between the other sectors (that is, drinking and, in the case of the Monte Cotugno reservoir, industrial). Downstream of the diversions, the volume of water left in the river (r^{env}_{t+1}) should ensure adequate environmental conditions to preserve fluvial ecosystems.

Moving from the single-reservoir model to a reservoir network, the scalar variables are replaced by vectors (boldface symbols, where Monte Cotugno = 1, Pertusillo = 2, Locone = 3, Conza = 4, Occhito = 5). For example, $\mathbf{s}_t$ contains all state variables of the system. Similarly, the operating policy is a vector function, $\mathbf{p}(\cdot)$, which produces the entire vector of decisions on the releases of the reservoirs ($\mathbf{u}_t$), together with an element representing the total amount of water drawn from the well fields (u^w_t).

Besides the decisions regarding the daily volumes of water released from reservoirs, extracted from wells, and allocated to various users, a key characteristic of each water portfolio is the strategic choice concerning the adoption of innovative water reuse technologies. Two configurations are considered: one reflecting the current state, in which no reuse interventions are implemented, and another that includes multiple reuse actions. The latter involves two wastewater reclamation plants capable of supplying a total of 61.97 Mm^3/year (49.36 Mm^3/year for agriculture and 12.61 Mm^3/year for industry). Additionally, up to 9.45 Mm^3/year can be recovered from seven well fields previously decommissioned due to groundwater quality concerns. A water portfolio is thus defined as an integrated management framework that combines operational aspects (such as the operations of reservoirs, wells, and diversions) with strategic reuse decisions (the adoption of water reuse technologies), enabling coordinated and system-wide optimization of water resources.

The water distribution system (WDS) is simulated using Aquator, a proprietary software developed by Water Resource Associates and Oxford Scientific Software Ltd used by AQP for the daily WDS operation. Aquator includes around 500 physical arcs (i.e., pipes and channels), each characterized by a certain flow, and around 250 nodes, in which the water balance is computed. Among the Aquator internal variables, we monitor the water flows supplied to the demand centers (i.e., the municipalities), $\mathbf{f}^{dri,d}_{t+1}$, to compute the drinking water deficits and those passing through some specific sections (withdrawals from wells, flow rates entering hydroelectric, pumping and purification plants), $\mathbf{f}^{dri,c}_{t+1}$, to estimate the water distribution cost.

The simulation of the system requires the definition of the scenario, i.e., the quantification of the whole set of input variables influencing the system's dynamics:

$$\omega = \{\mathbf{q}_{1,\dots,h}, \mathbf{w}^{irr}_{0,\dots,h-1}, \mathbf{w}^{ind}_{0,\dots,h-1}, \mathbf{w}^{dri}_{0,\dots,h-1}, \mathbf{c}^{dri}_{0,\dots,h-1}\}, \tag{B.3}$$

where $\mathbf{q}_{1,\dots,h}$ is the vector of all inflows, $\mathbf{w}^{irr}_{0,\dots,h-1}$, $\mathbf{w}^{ind}_{0,\dots,h-1}$ and $\mathbf{w}^{dri}_{0,\dots,h-1}$ are the water demand vectors, and $\mathbf{c}^{dri}_{0,\dots,h-1}$ represents the vector of all supply, treatment, and distribution costs per flow unit. Historical data (2010–2019) are used to define the baseline scenario, while the identification of robust water portfolios requires the generation of future projections.

The future hydro-meteorological variability is modeled using the projections from the IPCC Fifth Assessment Report. We select RCP 4.5 (a moderate climate change scenario), and RCP 8.5 (an extreme scenario) and two time horizons (2050–2059 and

2090–2099). An in-depth description of the hydrometeorological features of future scenarios is provided in Appendix C. Other than the climate aspects, future socio-economic evolution will impact the drinking water demand patterns. According to projections by the Apulian Water Authority, water demand along the coastline is expected to rise substantially, especially during the summer months, driven by tourism development. In contrast, certain rural areas are projected to see a decline in demand. The expected yearly increase in the drinking demand is 80.9 Mm^3 (approximately 17% of the current drinking demand).

The interest of the stakeholders is represented by a three-dimensional vector $\mathbf{J} = [J^{irr+ind}, J^{dri,d}, J^{dri,c}]$ of performance indicators to be minimized. Each objective represents the sum of averages over a ten-year horizon (h) of specific indicators in the different points of the system:

- Squared irrigation and industrial deficit,

$$J^{irr} = \frac{1}{h}\sum_{t=0}^{h-1}\sum_{i=1}^{N^{irr}}\left[\left(\max(\mathbf{w}_t^{irr}(i) - \mathbf{r}_{t+1}^{irr}(i),\ 0)\right)^2 + \left(\max(\mathbf{w}_t^{ind}(1) - \mathbf{r}_{t+1}^{ind}(1),\ 0)\right)^2\right], \tag{B.4}$$

  where $\mathbf{w}_t^{irr}(i)$ and $\mathbf{r}_{t+1}^{irr}(i)$ are the water demand and supply for the ith irrigation district. $\mathbf{w}_t^{ind}(1)$ and $\mathbf{r}_{t+1}^{ind}(1)$ are the water demand and supply relative to the only industrial district, linked to Monte Cotugno reservoir (index equal to 1).
- Potable water deficit,

$$J^{dri,d} = \frac{1}{h}\sum_{t=0}^{h-1}\sum_{i=1}^{N^{dri,d}}\left(\max(\mathbf{w}_t^{dri}(i) - \mathbf{f}_{t+1}^{dri,d}(i),\ 0)\right), \tag{B.5}$$

  where $\mathbf{w}_t^{dri}(i)$ and $\mathbf{f}_{t+1}^{dri,d}(i)$ are the demand and supply of the ith drinking demand center.
- Drinking water distribution cost,

$$J^{dri,c} = \frac{1}{h}\sum_{t=0}^{h-1}\sum_{i=1}^{N^{dri,c}}\mathbf{c}_t^{dri}(i)\cdot\mathbf{f}_{t+1}^{dri,c}(i), \tag{B.6}$$

  being $\mathbf{c}_t^{dri}(i)$ the cost per flow unit and $\mathbf{f}_{t+1}^{dri,c}(i)$ the flow relative to ith plant.

Due to the high computational effort required to run Aquator, $J^{dri,d}$ and $J^{dri,c}$ are directly computed using a high-fidelity and high-performing surrogate model Appendix A.

Appendix C. Future hydro-meteorological scenarios

The identification of robust water portfolios requires considering not only the historical conditions but also extending the analysis to a set of possible future scenarios that represent the expected variability of the processes at hand. In this appendix, we present the hydro-meteorological aspects of the future scenarios providing a detailed description of how they are generated starting from the climate projections. The daily water availability is defined by the inflows of the five considered reservoirs (Occhito, Conza, Locone, Pertusillo, and Monte Cotugno) and the streamflows of the two natural springs (Sele and Calore). Projections of these variables for the future periods that one wants to consider are necessary to simulate the strategic model.

IPCC projections of temperature and precipitation

We use the future climate scenarios provided by the Intergovernmental Panel on Climate Change (IPCC) in the fifth Assessment Report, which is a standard in the field of climate modeling and research. The IPCC report presents four Representative Concentration Pathways (RCP), each one describing a different climate depending on the greenhouse gas (GHG) concentration trajectory. Each RCP is labeled with its radiative forcing value in the year 2100 (2.6, 4.5, 6.0, and 8.5 W/m^2) and associated with an increase of the global surface temperature (with respect to the reference period 1850–1900). Temperature is expected to exceed 2 °C before the end of the 21st century in RCP 6.0 and RCP 8.5, and is more likely not to go beyond 2 °C in RCP 4.5. Conversely, in RCP 2.6 a temperature increase around 1 °C is expected. In our analysis, we consider RCP 4.5, which is described by the IPCC itself as an intermediate scenario, and RCP 8.5, an extreme scenario generally taken as the basis for worst-case analysis (in the last decade, RCP 8.5 has been thought to be very unlikely, but still possible).

Downscaling to the local scale

These future climate projections are generated at the global scale and used as input for global and regional models to generate variables such as temperature and rainfall. Since our strategic simulation model takes as input water flows in specific points of the region, it is first necessary to downscale the projections of temperature and precipitation to the local scale (local conditions for the historical period were derived from the E-OBS dataset, Cornes et al., 2018). This step is performed using quantile mapping, a traditional statistical downscaling technique used to remove possible systematic biases in global or regional circulation models (Enayati et al., 2021). Quantile mapping aims at finding a transformation that corrects the distribution of the large-scale variables so that it becomes as close as possible to that of the corresponding local-scale variables in the control (historical) period. Once the downscaling transformation is identified for the control period, it can be applied to correct the bias of the large-scale dataset in future periods as well.

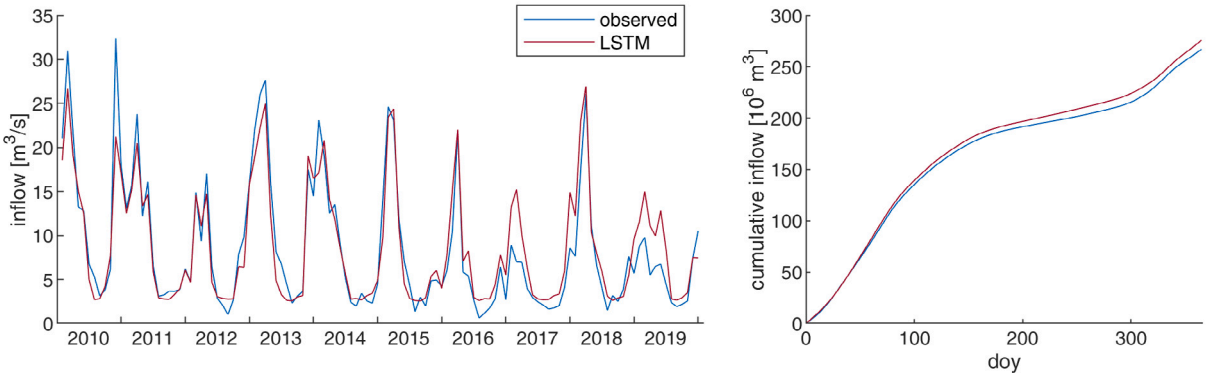

Fig. C.10. Comparison between observed and simulated trajectories of the inflow (left) and corresponding annual cumulative distribution (right). Pertusillo data are reported for the sake of example.

Table C.3
Mean yearly volumes [Mm^3/year] of reservoirs' inflow and natural springs' streamflow in the considered scenarios.

Variable	Baseline (2010–2019)	RCP 4.5 (2050–2059)	RCP 4.5 (2090–2099)	RCP 8.5 (2050–2059)	RCP 8.5 (2090–2099)
Occhito inflow	222.9	170.9	150.0	158.1	100.2
Locone inflow	36.7	31.3	28.9	29.9	22.6
Conza inflow	96.6	77.7	70.6	72.5	62.1
Pertusillo inflow	267.0	228.6	213.4	219.6	174.1
Monte Cotugno inflow	285.6	251.1	241.5	250.2	170.6
Calore streamflow	47.3	37.5	35.6	37.9	35.2
Sele streamflow	112.4	111.7	110.2	109.9	105.2
Overall water availability	1068.5	908.8	850.2	878.1	670.0

Hydrological projections at the basin scale

The downscaled projections of temperature and precipitation are then used to derive the corresponding water flows. This is usually done by feeding them into physically-based models, from basic rainfall-runoff models to more complex implementations involving several dynamics (such as those related to snowpack, glaciers, and soil moisture). However, the lack of reliable datasets for the area of interest in terms of temporal coverage and data quality prevents a satisfactory calibration of the parameters. In addition, the historical time series of the inflows is estimated by inverting the water-balance equation, thus deriving the net inflow (inflow minus the losses, such as evaporation). It can assume negative values, especially during summertime when evaporation is greater than the flow drained by the hydrological basin, which cannot be directly modeled with physically-based models, since they would require modeling the losses with specific sub-models (and thus also additional high-quality data).

For these reasons, we chose to directly derive the net inflow from temperature and rainfall following an empirical data-driven approach instead of the traditional physical one. We adopted recurrent neural networks (RNNs) made of long short-term memory (LSTM) cells (Hochreiter and Schmidhuber, 1997). Thanks to their internal memory and the gates that regulate the information flow inside the cells, LSTM nets are known to be more effective in tackling sequential tasks than traditional feed-forward (memoryless) networks and other ungated recurrent architectures (Han et al., 2004; Chandra and Zhang, 2012; Sangiorgio et al., 2021), though their training is computationally heavier (Goodfellow et al., 2016).

For each hydrological basin, we trained an LSTM network to reproduce the observed water flows (2010–19) feeding the model with the corresponding time series of temperature and rainfall. Fig. C.10 reports the comparison between observed (blue) and simulated (red) inflows of the Pertusillo reservoir in terms of daily trajectories (left panel) and cyclostationary cumulative distributions (right panel). It is important to emphasize that, more than the exact timing and punctual values, our model has to reproduce the statistical properties of the historical time series. The high similarity between observed and simulated cumulative distributions in all the considered basins ensures the goodness of the neural models identified.

Once the LSTM models have been identified on the historical data, they can be fed with future projections of temperature and precipitation that we previously downscaled to infer the future water availability in different periods and climate scenarios (Fig. C.11). Each panel is relative to a certain variable (temperature, rainfall, and inflow, along the rows) and climate scenarios (RCP 4.5 and 8.5, along the columns) and reports the comparison of the historical period (2010–2019, in blue), a mid-term future (2050–2059, red) and a long-term future (2090–2099, yellow).

In all the considered climate scenarios water availability is expected to decrease due to the concurrent effect of growing temperatures and decreasing precipitation (Table C.3). Two distinct clusters emerge. The first represents a moderate situation, RCP 4.5 and 8.5 by the middle of the 21st century, and RCP 4.5 from 2090–2099, which are associated with a reduction in water

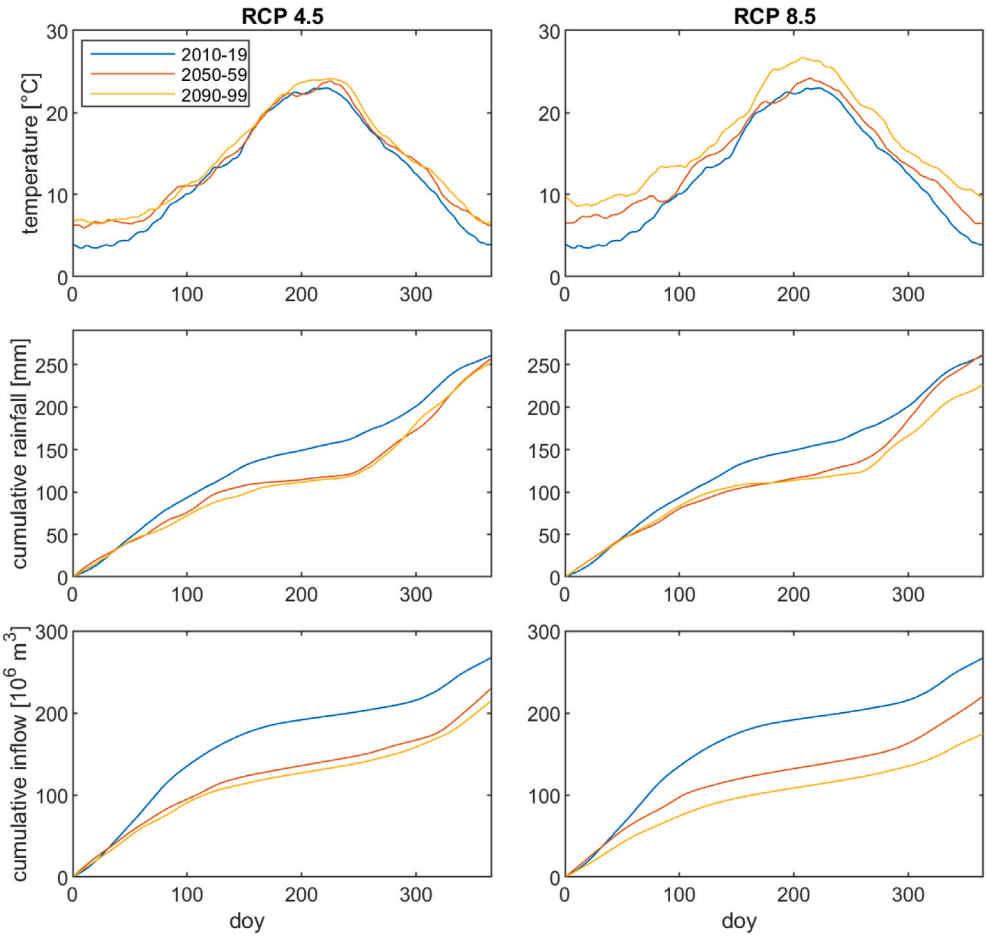

Fig. C.11. Cyclostationary time series of temperature, precipitation, and inflow for the Pertusillo reservoir. Each column is for a climate scenario (RCP 4.5 and 8.5), and each row is for a temporal horizon (2010–2019, 2050–2059, and 2090–2099).

availability of 14.9, 20.4, and 17.8% compared to the baseline. The second cluster coincides with RCP 8.5 at the end of the century and coincides with a loss of 398.5 Mm^3/year (37.3%).

This trend can be attributed to the fact that RCP 4.5 anticipates a stabilization of greenhouse gas emissions and, consequently, of the radiative forcing at 4.5 W/m^2 by the mid-century. RCP 8.5 follows a similar trajectory until mid-century (with radiative forcing hovering around 5 W/m^2 from 2050–2059) but continues to increase, reaching 8.5 W/m^2 by 2100 due to the absence of significant efforts to mitigate emissions.

Data availability

Data will be made available on request.

References

Ahmed, M., Mavukkandy, M.O., Giwa, A., Elektorowicz, M., Katsou, E., Khelifi, O., Naddeo, V., Hasan, S.W., 2022. Recent developments in hazardous pollutants removal from wastewater and water reuse within a circular economy. NPJ Clean Water 5 (1), 1–25.

Alhijawi, B., Awajan, A., 2024. Genetic algorithms: Theory, genetic operators, solutions, and applications. Evol. Intell. 17 (3), 1245–1256.

ARERA, 2020. Relazione Annuale: Volume 1 - Stato dei Servizi 2020. Technical Report, Autorità di Regolazione per Energia Reti e Ambiente.

Bertoni, F., Giuliani, M., Castelletti, A., 2020. Integrated design of dam size and operations via reinforcement learning. J. Water Resour. Plan. Manag. 146 (4), 04020010.

Büntgen, U., Urban, O., Krusic, P.J., Rybníček, M., Kolář, T., Kyncl, T., Ač, A., Koňasová, E., Čáslavskỳ, J., Esper, J., et al., 2021. Recent European drought extremes beyond Common Era background variability. Nat. Geosci. 14 (4), 190–196.

Cammalleri, C., Naumann, G., Mentaschi, L., Formetta, G., Forzieri, G., Gosling, S., Bisselink, B., De Roo, A., Feyen, L., 2020. Global warming and drought impacts in the EU. Publ. Off. Eur. Union: Luxemb..

Castelletti, A., Antenucci, J., Limosani, D., Quach Thi, X., Soncini-Sessa, R., 2011. Interactive response surface approaches using computationally intensive models for multiobjective planning of lake water quality remediation. Water Resour. Res. 47 (9).
Celeste, A.B., Billib, M., 2009. Evaluation of stochastic reservoir operation optimization models. Adv. Water Resour. 32 (9), 1429–1443.
Chandra, R., Zhang, M., 2012. Cooperative coevolution of elman recurrent neural networks for chaotic time series prediction. Neurocomputing 86, 116–123.
Chollet, F., et al., 2015. Keras. URL: https://github.com/fchollet/keras.
Commission for the Environment, Climate change and Energy, 2025. Turning the Tide – A Local and Regional Roadmap for Water Resilience. European Committee of the Regions, Opinion CDR-2276-2025, Rapporteurs: Kata Tüttő and Juanma Moreno.
Corbari, C., Paciolla, N., Restuccia, G., Al Bitar, A., 2024. Multi-scale EO-based agricultural drought monitoring indicator for operative irrigation networks management in Italy. J. Hydrol.: Reg. Stud. 52, 101732.
Cornes, R.C., Van Der Schrier, G., Van Den Besselaar, E.J., Jones, P.D., 2018. An ensemble version of the E-OBS temperature and precipitation data sets. J. Geophys. Res.: Atmos. 123 (17), 9391–9409.
De Girolamo, A., Barca, E., Leone, M., Porto, A.L., 2022. Impact of long-term climate change on flow regime in a Mediterranean basin. J. Hydrol.: Reg. Stud. 41, 101061.
Directorate-General for Environment, 2025. European Water Resilience Strategy. Technical Report, European Commission.
Enayati, M., Bozorg-Haddad, O., Bazrafshan, J., Hejabi, S., Chu, X., 2021. Bias correction capabilities of quantile mapping methods for rainfall and temperature variables. J. Water Clim. Chang. 12 (2), 401–419.
Essa, Y.H., Hirschi, M., Thiery, W., El-Kenawy, A.M., Yang, C., 2023. Drought characteristics in mediterranean under future climate change. Npj Clim. Atmos. Sci. 6 (1), 133.
EU Water Directors, 2016. Common Implementation Strategy for the Water Framework Directive and the Foods Directive: Guidelines on Integrating Water-reuse into Water Planning and Management in the Context of the WFD. Technical Report, European Commission.
Garrido-Perez, J.M., Vicente-Serrano, S.M., Barriopedro, D., García-Herrera, R., Trigo, R., Beguería, S., 2024. Examining the outstanding Euro-Mediterranean drought of 2021–2022 and its historical context. J. Hydrol. 630, 130653.
Giuliani, M., Lamontagne, J., Reed, P., Castelletti, A., 2021. A state-of-the-art review of optimal reservoir control for managing conflicting demands in a changing world. Water Resour. Res. 57 (12), e2021WR029927.
Giuliani, M., Mason, E., Castelletti, A., Pianosi, F., Soncini-Sessa, R., 2014. Universal approximators for direct policy search in multi-purpose water reservoir management: A comparative analysis. IFAC Proc. Vol. 47 (3), 6234–6239.
Giuliani, M., Quinn, J.D., Herman, J.D., Castelletti, A., Reed, P.M., 2017. Scalable multiobjective control for large-scale water resources systems under uncertainty. IEEE Trans. Control Syst. Technol. 26 (4), 1492–1499.
Giuliani, M., Zaniolo, M., Sinclair, S., Micotti, M., Van Orshoven, J., Burlando, P., Castelletti, A., 2022. Participatory design of robust and sustainable development pathways in the Omo-Turkana river basin. J. Hydrol.: Reg. Stud. 41, 101116.
Goodfellow, I., Bengio, Y., Courville, A., 2016. Deep Learning. MIT Press.
Guariso, G., Sangiorgio, M., 2019. Multi-objective planning of building stock renovation. Energy Policy 130, 101–110.
Guariso, G., Sangiorgio, M., 2020. Improving the performance of multiobjective genetic algorithms: An elitism-based approach. Information 11 (12), 587.
Hadka, D., Reed, P., 2013. Borg: An auto-adaptive many-objective evolutionary computing framework. Evol. Comput. 21 (2), 231–259.
Hamilton, A.L., Characklis, G.W., Reed, P.M., 2022. From stream flows to cash flows: leveraging evolutionary multi-objective direct policy search to manage hydrologic financial risks. Water Resour. Res. 58 (1), e2021WR029747.
Han, M., Xi, J., Xu, S., Yin, F.-L., 2004. Prediction of chaotic time series based on the recurrent predictor neural network. IEEE Trans. Signal Process. 52 (12), 3409–3416.
Han, Q., Xue, L., Liu, Y., Yang, M., Chu, X., Liu, S., 2023. Developing a multi-objective simulation-optimization model for ecological water conveyance in arid inland river basins. J. Hydrol.: Reg. Stud. 50, 101551.
Hatchard, S., Schmitt, R.J., Pianosi, F., Savage, J., Bates, P., 2023. Strategic siting and design of dams minimizes impacts on seasonal floodplain inundation. Environ. Res. Lett. 18 (8), 084011.
Hochreiter, S., Schmidhuber, J., 1997. Long short-term memory. Neural Comput. 9 (8), 1735–1780.
Hristov, J., Barreiro-Hurle, J., Salputra, G., Blanco, M., Witzke, P., 2021. Reuse of treated water in European agriculture: Potential to address water scarcity under climate change. Agricult. Water. Manag. 251, 106872.
Huang, J., Sangiorgio, M., Wu, W., Maier, H.R., Wang, Q.J., Hughes, J., Castelletti, A., 2025. Solving the robustness puzzle: The joint impact of optimization approach, robustness metrics, and scenarios on water resources management under deep uncertainty. J. Environ. Manag. 373, 123540.
Kahn, M., Sangiorgio, M., Rosa, L., 2025. Potential of wastewater reuse to alleviate water scarcity under future warming scenarios. Environ. Res. Lett. 20 (3), 034012.
Kingma, D.P., Ba, J., 2014. Adam: A method for stochastic optimization. arXiv preprint arXiv:1412.6980.
Lopez, A., Vurro, M., 2008. Planning agricultural wastewater reuse in southern Italy: The case of Apulia Region. Desalination 218 (1–3), 164–169.
Neri, A., Rizzuni, A., Garrone, P., Cagno, E., 2024. Barriers and drivers to the development of an effective water reuse chain: insights from an Italian water utility. Clean Technol. Environ. Policy 1–21.
Penserini, L., Moretti, A., Mainardis, M., Cantoni, B., Antonelli, M., 2024. Tackling climate change through wastewater reuse in agriculture: A prioritization methodology. Sci. Total Environ. 914, 169862.
Polemio, M., Lonigro, T., 2015. Trends in climate, short-duration rainfall, and damaging hydrogeological events (Apulia, Southern Italy). Nat. Hazards 75 (1), 515–540.
Quinn, J.D., Reed, P.M., Giuliani, M., Castelletti, A., 2019. What is controlling our control rules? Opening the black box of multireservoir operating policies using time-varying sensitivity analysis. Water Resour. Res. 55 (7), 5962–5984.
Razavi, S., Tolson, B.A., Burn, D.H., 2012. Review of surrogate modeling in water resources. Water Resour. Res. 48 (7).
Rizzo, L., Gernjak, W., Krzeminski, P., Malato, S., McArdell, C.S., Perez, J.A.S., Schaar, H., Fatta-Kassinos, D., 2020. Best available technologies and treatment trains to address current challenges in urban wastewater reuse for irrigation of crops in EU countries. Sci. Total Environ. 710, 136312.
Salazar, J.Z., Kwakkel, J.H., Witvliet, M., 2024. Evaluating the choice of radial basis functions in multiobjective optimal control applications. Environ. Model. Softw. 171, 105889.
Salazar, J.Z., Reed, P.M., Herman, J.D., Giuliani, M., Castelletti, A., 2016. A diagnostic assessment of evolutionary algorithms for multi-objective surface water reservoir control. Adv. Water Resour. 92, 172–185.
Sangiorgio, M., Cananzi, D., Weber, E., Salazar, J.Z., Castelletti, A., 2022. Surrogate modeling for water reuse planning in complex water systems. IFAC-PapersOnLine 55 (33), 111–116.
Sangiorgio, M., Dercole, F., Guariso, G., 2021. Forecasting of noisy chaotic systems with deep neural networks. Chaos Solitons Fractals 153, 111570.
Soncini-Sessa, R., Weber, E., Castelletti, A., 2007. Integrated and Participatory Water Resources Management-Theory. Elsevier.
Sun, R., Pan, B., Duan, Q., 2023. A surrogate modeling method for distributed land surface hydrological models based on deep learning. J. Hydrol. 624, 129944.
Todorovic, M., 2007. Monthly climatic water balance of the Apulia region (Southern Italy): analysis of historical weather data and the projections for the 21st Century. Clim. Water 462.
Valerio, C., Giuliani, M., Castelletti, A., Garrido, A., De Stefano, L., 2023. Multi-objective optimal design of interbasin water transfers: The Tagus-Segura aqueduct (Spain). J. Hydrol.: Reg. Stud. 46, 101339.
Zaniolo, M., Fletcher, S., Mauter, M.S., 2023. Multi-scale planning model for robust urban drought response. Environ. Res. Lett. 18 (5), 054014.